Insertion and Abstraction Pathways in the Reaction $O(^1D_2) + H_2 \rightarrow OH + H$

F. Javier Aoiz,[1] Luis Bañares,[1] Jesús F. Castillo,[1] Mark Brouard,[2] Wolfgang Denzer,[2] Claire Vallance,[2] Pascal Honvault,[3] Jean-Michel Launay,[3] Abigail J. Dobbyn,[4] and Peter J. Knowles[5]

[1]*Departamento de Química Física, Facultad de Química, Universidad Complutense, E–28040 Madrid, Spain*
[2]*The Physical and Theoretical Chemistry Laboratory, South Parks Road, Oxford, OX1 3QZ, United Kingdom*
[3]*PALMS, UMR 6627 du CNRS, Université de Rennes 1, Campus de Beaulieu, 35042 Rennes Cedex, France*
[4]*Department for Computation and Information, Daresbury Laboratory, Daresbury, Warrington, Cheshire WA4 4AD, United Kingdom*
[5]*School of Chemistry, University of Birmingham, Edgbaston, Birmingham B15 2TT, United Kingdom*

(Received 27 September 2000)

Rigorous quantum dynamical calculations have been performed on the ground $1\,^1A'$ and first excited $1\,^1A''$ electronic states of the title reaction, employing the most accurate potential energy surfaces available. Product rovibrational quantum state populations and rotational angular momentum alignment parameters are reported, and are compared with new experimental, and quasiclassical trajectory calculated results. The quantum calculations agree quantitatively with experiment, and reveal unequivocally that the $1\,^1A''$ excited state participates in the reaction.

DOI: 10.1103/PhysRevLett.86.1729 PACS numbers: 34.50.Lf, 34.50.Pi, 82.20.Pm

The quantitative theoretical description of bimolecular reactions has, to date, been possible only for very simple three-atom systems. Those best understood, namely the reactions $H + H_2$ [1] and $F + H_2$ [2], occur predominantly on ground electronic state potential energy surfaces (PESs) favoring direct scattering dynamics. Reactions proceeding over surfaces with deep potential energy wells, that may serve to trap reactive intermediates temporarily, have been more resistant to exact theoretical treatment. An important example is the insertion reaction

$$O(^1D_2) + H_2 \rightarrow OH(^2\Pi) + H\,, \qquad (1)$$

which has a potential energy minimum some 7 eV below the reactant asymptote.

Reaction (1) is complicated further by the presence of five PESs correlating with the $O(^1D_2)$ reactants. Although all five PESs are Coriolis-coupled in the entrance channel [3], leading to scrambling of any O atom electronic orbital alignment [3], reactivity is dominated by the highly attractive ground $1\,^1A'$ state, and by the first two excited states $1\,^1A''$ and $2\,^1A'$, whose participation in the reaction has been hotly debated (see [3–7], and references therein). Reactive scattering over the $1\,^1A''$ PES surface, which correlates adiabatically from ground state reactants to products and has a barrier of 100 meV, exhibits direct rebound dynamics reminiscent of the $F + H_2$ reaction. Unlike reaction on the $1\,^1A'$ PES, which generates OH products distributed near-statistically over all accessible rovibrational levels, reaction on the excited $1\,^1A''$ PES leads to a highly inverted OH vibrational population distribution [5]. The reactivity of the $2\,^1A'$ PES, in contrast, which correlates with electronically *excited* $OH(A^2\Sigma) + H$ products, is governed by nonadiabatic coupling via a conical intersection with the ground $1\,^1A'$ state. Nonadiabatic reaction involving this $2\,^1A'$ surface generates OH population distributed over the full range of accessible product quantum states, and, as a consequence, evidence for its involvement in the $O(^1D_2) + H_2$ system is likely to prove hard to find at collision energies around 100 meV.

In this Letter we present the results of a combined experimental and theoretical study, which uses OH quantum state-resolved populations and rotational angular momentum alignment (i.e., the alignment of the OH rotational angular momentum vector $\mathbf{j}'$ with respect to the reagent relative velocity $\mathbf{k}$) to test rigorously current understanding of reaction (1). We focus on those specific products which bear clearest witness to the involvement of the $1\,^1A''$ excited state, namely those generating $OH(v' = 3, 4, j')$, and compare the experimental results with *exact* adiabatic quantum mechanical (QM) and quasiclassical trajectory (QCT) scattering calculations on the best available $1\,^1A'$ and $1\,^1A''$ PESs. To our knowledge, the QM calculations on the $1\,^1A'$ PES constitute the largest accurate scattering calculation ever performed for an atom-diatom reaction.

The scattering calculations were performed on PESs derived from accurate *ab initio* electronic structure computations [8]. Internally contracted multireference configuration interaction wave functions [9] with large orbital basis sets and flexible reference wave functions covering all important valence and Rydberg configurations were computed at around 1000 geometries for each of the $\tilde{X}(^1A_1, ^1A')$, $\tilde{A}(^1B_1, ^1A'')$ and $\tilde{B}(^1A_1, ^1A')$ states. The adiabatic PESs were then transformed to a diabatic Hamiltonian matrix through an approximate diabatization of the $\tilde{X}$ and $\tilde{B}$ states based on their transition angular momentum matrix elements with the $\tilde{A}$ state [10], and the resulting diabatic functions fitted to a three-dimensional analytic form. The final analytic adiabatic surfaces, denoted DK in what follows, were then recovered by diagonalization of the $2 \times 2\,^1A'$ Hamiltonian matrix.

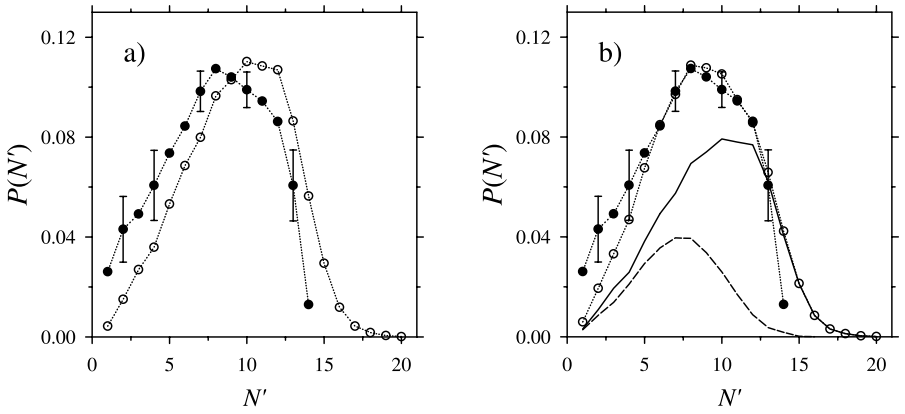

FIG. 1. Comparison between the experimental rotational populations for the OH($v' = 4$) products (solid circles with error bars) with those derived from the QM calculations on the $1\,^1A'$ DK PES alone (a), or from those including contributions from both the $1\,^1A'$ and $1\,^1A''$ DK PES (b). In (b), the continuous solid line represents the contribution from the A' PES, while that from the A'' PES is shown as a dashed line.

The QM reactive scattering calculations on the $1\,^1A'$ DK PES employed a time-independent method, and body-frame democratic hyperspherical coordinates [11,12] to represent the nuclear wave function. First a set of eigenstates of a simplified Hamiltonian $H_0 = T + V$ were determined, where V is the potential energy, and T the kinetic energy arising from deformation and rotation around the principal axis of least inertia at fixed hyperradius. The full scattering wave function, which is the solution of the exact Hamiltonian, is then expanded in a basis of eigenstates of H_0 that dissociate at large hyperradius into the H_2 $(14, 12, 8, 2)$ and OH $(40, 38, 36, 33, 30, 28, 24, 21, 17, 11)$ rovibrational sets (this notation indicates the largest rotational level j for each vibrational manifold). The expansion coefficients are the solutions of a set of second order differential equations with couplings arising from the difference between the exact Hamiltonian and H_0. No restrictions were placed on the helicity quantum number k (the projection of the total angular momentum J of the system on each of the atom-diatom axes). Thus $k_{\max} = J$ and the number of coupled equations increases from 310 for $J = 0$ to 4505 for $J = 25$. The S matrix and several observables, such as integral cross sections, were computed for the $O(^1D) + H_2(v = 0, j = 0)$ reaction at the collision energies 25, 56, and 100 meV.

The QM calculations on the $1\,^1A''$ DK PES employed the CCP6 reactive scattering program [13], which uses the same methods previously employed in studies of $F + H_2$(HD) [2]. Calculations were performed for $O(^1D) + H_2(v = 0, j = 0, 1)$ at the collision energies 80, 100, 120, 160, and 200 meV. All reactant and product channels with diatomic rotational quantum number $j_{\max} = 22$, $k_{\max} = 3$, and internal energies $E_{\max} = 1.4$ eV were included in the basis set. Calculations with $J \leq 28$ were necessary to obtain well-converged results.

The QCT calculations were performed by running batches of 400 000 and 550 000 trajectories on the $1\,^1A'$ and $1\,^1A''$ DK PESs, sampling the collision energy range 5–400 meV and $H_2(v = 0)$ reactants in rotational levels $j = 0$–3 [14]. The calculation of both the QM and QCT rotational alignment parameters $a_0^{(2)}$ was carried out as described in Ref. [15] in which the classical and quantum descriptions of the stereodynamics of atom-diatom reactions were presented.

$O(^1D_2)$ atoms were generated experimentally by polarized 193 nm pulsed laser photolysis of N_2O in a flowing 50:50 gas mixture with H_2, held at a 100 mtorr pressure and a temperature of 300 K [4,16]. The OH($v' = 3, 4$) reaction products were probed at a time delay of $\sim$100 ns by laser induced fluorescence (LIF) on the $1 \leftarrow 4$ and $0 \leftarrow 3$ vibronic bands of the $A \leftarrow X$ transition, using polarized dye laser radiation ($\sim$0.2 cm^{-1} bandwidth) centered around $\lambda \sim 450$ nm. OH(A) emission was detected through a 310 nm (FWHM = 25 nm) interference filter using a photomultiplier. To obtain quantum state populations, the transition intensities were corrected for Einstein B coefficients, OH(A) predissociation rates [17], and detector sensitivity. An average of four spectra per rotational branch were used to determine the rotational populations, which have been summed over OH spin-orbit and Λ-doublet levels.

TABLE I. The experimental vibrational population ratio $P(v' = 4)/P(v' = 3)$ compared with those obtained using either QM [22] or QCT methods. The two sets of calculations are either for the ground $1\,^1A'$ DK PES alone, or for the summed adiabatic contributions from the $1\,^1A'$ and $1\,^1A''$ DK PESs. Errors are 2σ.

	$P(v' = 4)/P(v' = 3)$
Experiment	0.63 ± 0.05
QM $A' + A''$	0.61
QCT $A' + A''$	0.60 ± 0.01
QM A'	0.53
QCT A'	0.47 ± 0.01

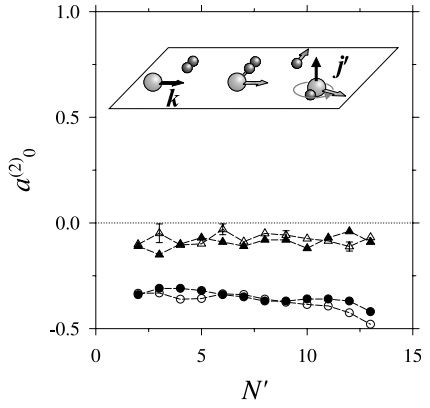

FIG. 2. Comparison between the QM (filled symbols) and QCT (open symbols) calculated alignment parameters as a function of j' for the OH($v' = 4$) products of the $O(^1D_2) + H_2(v = 0, j = 0)$ reaction at a fixed collision energy of 100 meV. Triangles and circles, calculations on the $1\,^1A'$ and $1\,^1A''$ DK PES, respectively. Note that in the classical limit $a_0^{(2)} = \langle P_2(\hat{\mathbf{k}} \cdot \hat{\mathbf{j}}')\rangle$. The inset illustrates the OH rotational motion generated on the $1\,^1A''$ PES.

OH rotational alignment parameters were determined on selected transitions from the ratio of LIF intensities recorded in two counterpropagating laser geometries [16,18]. The intensity data were used to determine laboratory frame rotational alignments $A_0^2(\mathrm{LAB})$ using the line-strength expressions given in Ref. [19]. $A_0^2(\mathrm{LAB})$ parameters were then transformed into the center-of-mass frame via the equation $A_0^2(\mathrm{LAB}) = \frac{4}{5}\langle P_2(\hat{\boldsymbol{\mu}} \cdot \hat{\mathbf{k}})\rangle a_0^{(2)}$, where $\langle P_2(\hat{\boldsymbol{\mu}} \cdot \hat{\mathbf{k}})\rangle$ is the second Legendre moment of the angular distribution of $\mathbf{k}$ about $\boldsymbol{\mu}$, the N_2O photolysis transition moment [4,16]. Under the experimental collision energy conditions (discussed below) $\langle P_2(\hat{\boldsymbol{\mu}} \cdot \hat{\mathbf{k}})\rangle$ was calculated to be 0.15 ± 0.01 [16], assuming an N_2O translational anisotropy parameter $\beta = 0.48 \pm 0.02$ [20].

The experimental $O(^1D_2)$ atom source generates a distribution of collision energies, with a mean of 120 meV and FWHM of 160 meV [4,20,21]. This distribution was calculated from the known speed distribution of the $O(^1D_2)$ atoms [20], taking into account the 300 K thermal motion of the N_2O precursor and H_2 target molecules [21]. To make a proper comparison with the experiments, the QM and QCT results have been averaged over the experimental collision energy distribution [22]. We emphasize, however, that the general conclusions drawn below are also reached if the experimental results are compared with calculated QM data for $H_2(j = 0)$ at a *fixed* 100 meV collision energy, which is close to the experimental mean.

The experimental rotational populations for the OH($v' = 4$) products of reaction (1) are compared with those derived from the QM calculations in Fig. 1. Two sets of theoretical data are shown: in Fig. 1(a) scattering over the ground $1\,^1A'$ state surface *alone* is considered, while in Fig. 1(b), contributions from reaction on both the $1\,^1A'$ and $1\,^1A''$ PESs are included. The latter calculations agree significantly better with experiment. The corresponding QCT distributions (not shown) are qualitatively the same as those calculated *via* QM methods, but are shifted one or two quanta towards higher N'. The OH vibrational population ratios, $P(v' = 4)/P(v' = 3)$, shown in Table I, also indicate that reaction over the excited $1\,^1A''$ state PES must be considered. Because reaction over the $1\,^1A''$ PES preferentially yields vibrationally excited OH molecules, the calculated $P(v' = 4)/P(v' = 3)$ ratio is larger when the A'' PES is taken into account: only if the latter contribution is included can quantitative agreement with the experiments be obtained.

Figure 2 compares QCT and QM calculated OH($v' = 4, j'$) rotational alignment parameters $a_0^{(2)}$ generated by reaction over the $1\,^1A'$ and $1\,^1A''$ DK PESs. The calculations are for $O(^1D) + H_2(v = 0, j = 0)$ at a collision energy of 100 meV. Unlike the population data, the agreement between the QM and QCT calculated alignment parameters is excellent. The theoretical $a_0^{(2)}$ values obtained for

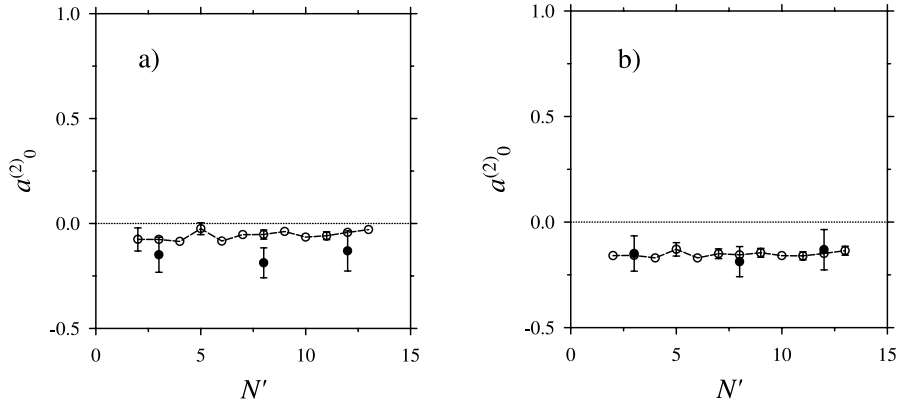

FIG. 3. Comparison of the experimental alignment parameters for the OH($v' = 4$) products (solid circles with error bars) with those derived from QCT calculations on the $1\,^1A'$ DK PES alone (a), and with those including contributions from both the $1\,^1A'$ and $1\,^1A''$ DK PES (b). The QCT data have been fully averaged over the experimental collision energy and reagent H_2 rotational distributions.

reaction over the excited $1\,^1A''$ PES are close to the limiting value of $-\frac{1}{2}$, indicating a strong propensity for $\mathbf{j}' \perp \mathbf{k}$ (see the inset to Fig. 2). Scattering over the $1\,^1A'$ PES is seen to generate much weaker OH alignment. The experimentally determined $a_0^{(2)}$ parameters are compared with those calculated using QCT methods in Fig. 3. Theoretical results are again shown either for reaction exclusively on the ground $1\,^1A'$, or for reaction over both $1\,^1A'$ and $1\,^1A''$ DK PESs. It is apparent once more that excellent agreement between theory and experiment is obtained once the contribution from the excited $1\,^1A''$ DK PES is included.

All the evidence presented here suggests that the excited $1\,^1A''$ PES plays an observable role in the $O(^1D) + H_2$ reaction at the collision energies sampled by the experiments. Moreover, the state-of-the-art QM scattering calculations indicate that the DK versions of the PESs are sufficiently accurate to allow quantitative modeling of the experimental results. Although further work on the effects of nonadiabatic scattering would clearly be desirable [3], the excellent agreement between experiment and theory presented here suggests that they have a very minor influence on the properties of reaction (1) investigated here.

We gratefully acknowledge fruitful discussions with John P. Simons. The experimental work was supported by the EPSRC (GR/L 97339) and the Leverhulme Trust (F788). The QCT calculations, and the QM calculations on the DK A'' PES were performed on a SG Origin 2000 of the "Centro de Supercomputación Complutense" and funded by Grant No. DGICYT PB98-0762-C03-01. EU support (to M. B. and F. J. A.) through the RTN project HPRN-CT-1999-00007 is also acknowledged. The QM calculations on the $1A'$ PES were performed on a NEC-SX5 vector supercomputer, through a grant from the "Institut du Développement des Ressources en Informatique Scientifique" (IDRIS) in Orsay (France).

[1] L. Schnieder, K. Seekamp-Rahn, E. Wrede, and K. H. Welge, J. Chem. Phys. **107**, 6175 (1997), and references therein.

[2] R. T. Skodje, D. Skouteris, D. E. Manolopoulos, S.-H. Lee, F. Dong, and K. Liu, Phys. Rev. Lett. **85**, 1206 (2000), and references therein.

[3] K. Drukker and G. C. Schatz, J. Chem. Phys. **111**, 2451 (1999); S. K. Gray, C. Petrongolo, K. Drukker, and G. C. Schatz, J. Phys. Chem. A **103**, 9448 (1999).

[4] A. J. Alexander, D. A. Blunt, M. Brouard, J. P. Simons, F. J. Aoiz, L. Bañares, Y. Fujimura, and M. Tsubouchi, Faraday Discuss. Chem. Soc. **108**, 375 (1997).

[5] F. J. Aoiz, L. Bañares, M. Brouard, J. F. Castillo, and V. J. Herrero, J. Chem. Phys. **113**, 5339 (2000).

[6] A. J. Alexander, F. J. Aoiz, L. Bañares, M. Brouard, and J. P. Simons, Phys. Chem. Chem. Phys. **2**, 571 (2000).

[7] X. Liu, J. J. Lin, S. Harich, G. C. Schatz, and X. Yang, Science **289**, 1536 (2000).

[8] A. J. Dobbyn and P. J. Knowles (to be published). Copies of the surfaces may be downloaded from the web site http://www.tc.bham.ac.uk/~peterk/h2osurface

[9] H.-J. Werner and P. J. Knowles, J. Chem. Phys. **89**, 5803 (1988).

[10] A. J. Dobbyn and P. K. Knowles, Mol. Phys. **91**, 1107 (1997).

[11] J.-M. Launay and M. Le Dourneuf, Chem. Phys. Lett. **163**, 178 (1989); **169**, 473 (1990); B. Lepetit and J.-M. Launay, J. Chem. Phys. **95**, 5159 (1991).

[12] P. Honvault and J.-M. Launay, Chem. Phys. Lett. **287**, 270 (1998); **303**, 657 (1999); J. Chem. Phys. **111**, 6665 (1999).

[13] D. Skouteris, J. F. Castillo, and D. E. Manolopoulos, Comput. Phys. Commun. **133**, 128 (2000); http://www.dl.ac.uk/CCP/CCP6/library.html

[14] F. J. Aoiz, L. Bañares, and V. J. Herrero, J. Chem. Soc. Faraday Trans. **94**, 2483 (1998).

[15] M. P. de Miranda, F. J. Aoiz, L. Bañares, and V. Sáez Rábanos, J. Chem. Phys. **111**, 5368 (1999).

[16] M. Brouard, S. D. Gatenby, D. M. Joseph, and C. Vallance, J. Chem. Phys. **113**, 3162 (2000).

[17] *LIFBASE: Database and simulation program (v. 1.6).* J. Luque and D. R. Crosley, SRI International Report MP No. 99-009 (1999).

[18] M. P. Docker, Chem. Phys. **135**, 405 (1989).

[19] C. H. Greene and R. N. Zare, J. Chem. Phys. **78**, 6741 (1983).

[20] P. Felder, B.-M. Haas, and J. R. Huber, Chem. Phys. Lett. **186**, 177 (1991).

[21] M. Brouard, S. P. Duxon, P. A. Enriquez, and J. P. Simons, J. Chem. Phys. **97**, 7414 (1992).

[22] To perform the averaging over the experimental collision energy distribution, which spans the range $\sim$0–200 meV, the QM data on the $1\,^1A'$ DK PES, which are only available at energies $\leq$100 meV, have been extrapolated carefully using scaled QCT results calculated over the energy grid 5–400 meV. Note also that we have equated $N' = j' + 1$, where j' is the pure rotational angular momentum of the nuclei used in the calculations, and N' is the total OH angular momentum apart from electron spin used experimentally.